Journal Pre-proofs

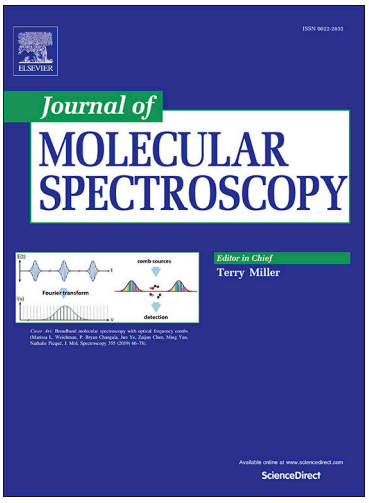

High-Resolution spectroscopy of the [18.4]2.5 – $X^2\Delta_{5/2}$ transition of ruthenium monoboride (RuB)

J.M. Dore, A.G. Adam, C. Linton, D.W. Tokaryk

PII: S0022-2852(20)30089-8
DOI: https://doi.org/10.1016/j.jms.2020.111321
Reference: YJMSP 111321

To appear in: *Journal of Molecular Spectroscopy*

Received Date: 28 April 2020
Revised Date: 2 June 2020
Accepted Date: 8 June 2020

Please cite this article as: J.M. Dore, A.G. Adam, C. Linton, D.W. Tokaryk, High-Resolution spectroscopy of the [18.4]2.5 – $X^2\Delta_{5/2}$ transition of ruthenium monoboride (RuB), *Journal of Molecular Spectroscopy* (2020), doi: https://doi.org/10.1016/j.jms.2020.111321

High-Resolution spectroscopy of the [18.4]2.5 – $X^2\Delta_{5/2}$ transition of ruthenium monoboride (RuB).

J.M. Dore[a], A.G. Adam[a], C. Linton[b*], D.W. Tokaryk[b]

[a] Department of Chemistry and Centre for Laser, Atomic, and Molecular Sciences, University of New Brunswick, Fredericton, New Brunswick E3B 5A3, Canada

[b] Department of Physics and Centre for Laser, Atomic, and Molecular Sciences, University of New Brunswick, Fredericton, New Brunswick E3B 5A3, Canada

*Corresponding author: e-mail address: colinton@unb.ca (C. Linton)

Abstract:

Laser-induced fluorescence spectra of the (0, 0), (1, 0) and (0, 1) bands of the [18.4]2.5 – $X^2\Delta_{5/2}$ transition have been recorded at high - resolution for several isotopologues of ruthenium monoboride (RuB). We report band origins and rotational parameters for 12 of the 14 possible isotopologues (7 for each of $Ru^{11}B$ and $Ru^{10}B$) as well as hyperfine parameters of ^{99}RuB and ^{101}RuB. An anomalous isotope shift in the (0, 0) and (0, 1) bands indicates a weak perturbation in the [18.4]2.5 v = 0 vibrational level. The observed hyperfine structure is mainly due to the nuclear spin (I = 5/2) of the two Ru isotopes. Hyperfine structure due to the ^{11}B and ^{10}B isotopes was not resolved and resulted in, at most, a slight broadening of the lines. The magnetic hyperfine parameters help to confirm the $(11\sigma)^2(5\pi)^4(2\delta)^3$ configuration of the ground electronic state and provide insight into the configuration of the excited states.

1. Introduction

Transition metal (TM) borides are regarded as refractory compounds and possess many remarkable physical properties such as exceptional corrosion resistance and super hardness (ReB_2) [1]. Many TM borides are known to be good catalysts for hydrogenation of alkenes and alkynes, reduction of nitrogenous functional groups, and deoxygenation reactions [2]. In addition, ruthenium-containing compounds have long been known as effective catalysts for a variety of chemical reactions such as the Fischer-Tropsch synthesis for hydrocarbon chains [3], oxidations of alcohols [4], olefin metathesis [5], and ring-opening metathesis [6]. As a result, ruthenium catalysts play a key role in organic and pharmaceutical industries. Recently, and pertinent to this work, thin-films of ruthenium boride created through laser deposition show extreme hardness similar to that of rhenium diboride, and are of interest in industrial applications ranging from cutting tools to wear resistant surfaces [7].

The catalytic and physical properties of ruthenium-containing compounds and TM borides described above prompt further investigation into the nature of their chemical bonding and electronic structure. In a recent publication [8], we described how analysis of the rotational and hyperfine structure in high-resolution laser induced fluorescence (LIF) spectra of cobalt monoboride, CoB, provided insight into the bonding and configurational composition of the electronic states. In this paper, we present a study, similar to that of CoB [8], of the high-resolution spectroscopy of ruthenium monoboride, RuB, using a laser ablation/reaction free jet expansion technique in conjunction with LIF spectroscopy. Theoretical calculations of the molecular properties of the ground state of RuB using density functional theory (DFT) have been performed by Kharat et al. [9] who predicted a bond length of r_e=1.761 Å and vibrational frequency ω_e=910.8 cm^{-1}. Experimentally, Wang et al. [10] used pulsed lasers to obtain medium-resolution LIF spectra and rotationally analyze three vibronic bands of RuB which were identified as the (1,0) (0,0) and (0,1) bands of the [18.4]2.5 - $X^2\Delta_{5/2}$ system. They were able to distinguish and analyze spectra of the $Ru^{11}B$ and $Ru^{10}B$ isotopologues but were unable to resolve any of the 7 naturally occurring Ru isotopes. Their rotational constants of $Ru^{11}B$ and $Ru^{10}B$ are therefore isotopically-averaged values. Their experimentally determined bond length r_0"=1.7099 Å of the ground state differs from the predicted value by Kharat et al. [9], but the experimental vibrational frequency $\Delta G_{1/2}$=911.02 cm^{-1} is in agreement with the DFT calculations. In this paper, we report results of the first high-resolution study of RuB. Rotational analysis was performed on 12 of the possible 14 isotopologues of RuB improving upon the existing molecular constants by an order of magnitude. In addition, hyperfine structure was resolved and the magnetic hyperfine constants of the [18.4]2.5 and $X^2\Delta_{5/2}$ states were determined for the odd isotopes of Ru (^{101}Ru and ^{99}Ru). The hyperfine analysis of RuB

helped confirm the $^2\Delta_i$ ground state symmetry and provides some insight into the excited state electronic configuration.

2. Experimental

The molecular production scheme is identical to that used in the recent study of CoB [8] except that a rubidium rather than cobalt rod was ablated with ~7 mJ of 355 nm radiation from a Nd:YAG laser to vaporize Ru atoms for the reaction with B_2H_6 to produce RuB. For the high-resolution spectra, a Coherent 699-21 cw-ring dye laser pumped by an argon ion laser at wavelengths of 488 and 514.5 nm was used. Coumarin 521, Rhodamin 110 and R6G dyes were used in the wavelength region from 520-575 nm containing the (1, 0), (0, 0) and (0, 1) vibrational bands. All other details such as conditions for medium – resolution survey scans, gas mixture, data collection and calibration are the same as those described in [8].

Typical linewidths (FWHM) obtained for unblended high-resolution spectral lines are approximately 120 MHz. Linewidths of the ^{101}RuB and ^{99}RuB isotopologues are larger because of partially resolved or unresolved hyperfine structure due to the ^{101}Ru and ^{99}Ru nuclear spin, I = 5/2.

3. Observations and Analysis

Medium-resolution:

The medium-resolution LIF spectrum of RuB, shown in Figure 1, was recorded in the region between 420 and 675 nm. Six bands, at 471 nm 487 nm 505 nm 523 nm 542 nm and 570 nm, were observed and assigned as the (4, 0), (3, 0), (2, 0), (1, 0), (0, 0) and (0, 1) bands respectively of the [18.4]2.5-$X^2\Delta_{5/2}$ electronic system as shown. The upper state vibrational intervals, ~665 - 670 cm^{-1}, are irregular and the data do not lend themselves to a meaningful fit. In addition, several other bands are observed that do not fit in to the present band system and whose origin and assignment are presently unknown.

Dispersed Fluorescence:

Fig. 2 shows dispersed fluorescence spectra (DFs) taken with the pulsed laser exciting the (1, 0) band heads of each of the $Ru^{11}B$ and $Ru^{10}B$ isotopologues which were clearly separated in the medium – resolution spectrum in fig. 1. The DFs show fluorescence to the v = 0 – 5 vibrational levels of the ground state and clearly show the larger vibrational spacing in the $Ru^{10}B$ isotopologue. There was also fluorescence (labelled by asterisks in fig, 2) at 5996 cm^{-1} above the ground v = 0 level which was the same for both isotopologues and probably involved a transition to the v = 0 level of a different low-lying electronic state.

The vibrational energies, relative to the v = 0 level, obtained from the DF data are displayed in Table 1 which also lists the $Ru^{11}B$ and $Ru^{10}B$ ground state vibrational constants obtained from a least-squares fit to the energies.

High-resolution:

Only the three previously reported (1, 0), (0, 0) and (0, 1) bands [10] were obtained at high-resolution in our study as the other transitions occurred at wavelengths for which the power of the cw-ring dye laser was poor. As pointed out in the introduction, the previous rotational analysis of these bands failed to resolve the spectra of the ruthenium isotopes resulting in $Ru^{11}B$ and $Ru^{10}B$ constants which were averaged over the Ru isotopes.

Ruthenium has 7 naturally occurring isotopes: ^{104}Ru(18.6%), ^{102}Ru(31.6%), ^{101}Ru (17.1%), ^{100}Ru(12.6%), ^{99}Ru(12.8%), ^{98}Ru(1.9%) and ^{96}Ru(5.5%). Using the cw ring dye laser, the above three bands of the [18.4]2.5-$X^2\Delta_{5/2}$ system were recorded at high-resolution and the (0, 0) and (1, 0) bands of 12 of the 14 possible RuB isotopologues were rotationally analyzed. The ^{98}RuB isotopologue was too weak to be observed. Fig. 3 shows the lowest rotational transitions in the Q branch of the (1, 0) band in which the Ru isotope structure is clearly observed. Because of the low

population of the v″ = 1 level in the cold molecular beam, the (0, 1) band was very weak and only the $^{104}Ru^{11}B$, $^{102}Ru^{11}B$ and $^{100}Ru^{11}B$ isotopologues were observed and analyzed. Transitions up to J'' = 12.5 were observed. The assignment of the rotational structure was fairly straight forward. The *P*, *Q* and *R* branches were easily identified, and the most intense series in each branch were assigned to the ^{102}RuB isotopologue. Scaling the ^{102}RuB combination differences using the inverse reduced mass dependence helped to assign the other isotopic series in each branch. Because of the overlap with the more intense $Ru^{11}B$ lines in the (0, 0) band and the low intensity of the (0, 1) band, the weak $Ru^{10}B$ lines were sufficiently separated from $Ru^{11}B$ and intense enough to be analyzed only for the (1, 0) band. The first rotational transitions in each branch were found to be *P*(3.5), *Q*(2.5) and *R*(2.5), as previously reported [10], confirming the ground state symmetry as $^2\Delta_{5/2}$ and the upper state as Ω = 2.5. No hyperfine structure was observed for the isotopologues of the even-mass Ru isotopes which have no nuclear spin and the term energies of the two states were fitted to the standard polynomial expression

$$T(\mathrm{v,J}) = T_0 + B\mathrm{x} - D\mathrm{x}^2 \qquad (1)$$

where $\mathrm{x} = [J(J+1) - \Omega^2]$.

For each isotopologue, the bands were first fitted individually to check for bad assignments and perturbations and then all together in a global fit whose results are presented in Tables 2 and 3 for $Ru^{11}B$ and $Ru^{10}B$ respectively.

Fig. 3 also illustrates the hyperfine broadening and splitting of the rotational lines in the ^{101}RuB and ^{99}RuB isotopologues which are caused primarily by the nuclear spin, I = 5/2, of each of the ^{101}Ru and ^{99}Ru isotopes. This is expanded in fig. 4 to show the detailed hyperfine structure in the *Q*(2.5) transition of the (1, 0) band of the $^{101}Ru^{11}B$ isotopologue. The hyperfine structure is not completely resolved. The six main transitions with $\Delta F = \Delta J = 0$ are the most intense and are

accompanied by weaker $\Delta F \neq \Delta J$ satellite transitions with $\Delta F = \pm 1$ for a Q branch. There is considerable overlap between the main and satellite transitions as shown in fig. 4. The lower spectrum is a PGOPHER [11] simulation using the constants (table 2) obtained from a fit to the data and is seen to reproduce the observed spectrum very well. For the R and P branches the satellite transitions would have $\Delta F = 0$.

The magnetic hyperfine term energies, which are added to the rotational term energies in eq. 1, are given primarily by the diagonal term in the Hamiltonian matrix

$$W_{mhf} = \frac{h_\Omega \Omega C}{(2J(J+1))} \quad (2)$$

where $$C = F(F+1) - J(J+1) - I(I+1) \quad (3)$$

and $$h_\Omega = a\Lambda + (b_f + 2c/3)\Sigma \quad (4)$$

The present data are insufficient to determine the Frosch and Foley hyperfine parameters [12], a, b_f and c. The only hyperfine parameter that can be determined directly from a fit to the data is h_Ω. This is discussed further below. The off-diagonal $\Delta F = 0$, $\Delta J = \pm 1$ contributions to the hyperfine energy [13] turned out to be very small but were included in the final least squares fit to the data. The quadrupole hyperfine terms were found to be negligible and only the magnetic hyperfine structure was significant. The final parameters, including h_Ω, are presented in Tables 2 and 3.

4. Discussion

(a) Vibration:

In Tables 2 and 3, the [18.4]2.5 state T values for $v' = 0$ and 1 are the band origins, T_{00} and T_{10}, of the (0, 0) and (1, 0) bands. The band origins of the (0, 1) band in Table 2 are given by subtracting the listed $X^2\Delta_{5/2}$ state $v'' = 1$ energies from those of the [18.4]2.5 state $v' = 1$ ie $T_{01} = T_{0'} - T_{1''}$. Precise observed vibrational intervals, $\Delta G_{1/2}$, for all $^{i}Ru^{11}B$ isotopologues in the excited state and for the even mass i = 104, 102 and 100 isotopologues in the ground state were calculated from

the band origins and are listed in Table 4. Also shown are the ratios of the $\Delta G_{1/2}$ values relative to that of $^{104}Ru^{11}B$ and the inverse reduced mass ratio $\rho = (\mu_{104}/\mu_i)^{1/2}$. The agreement between the observed ratios and ρ is excellent for the ground state and poor for the excited state. This indicates that the ground state is probably regular and unperturbed and that there are perturbations or interactions affecting the [18.4]2.5 state. This can be investigated further by examining the isotope shifts in the vibrational levels of the various isotopologues.

In Tables 2 and 3, the listed energy, T, of the upper state $v' = 0$ level is observed to increase as the Ru mass decreases. As the term energy of the ground state, $v'' = 0$ level was set at zero for each RuB isotopologue, T actually represents the difference between the upper and ground state term energies $T_{v'}$ and $T_{0''}$ respectively. i.e.

$$T = T_{v'} - T_{0''}$$

The energy of each vibrational level is expected to increase with decrease in the isotope mass and, as the vibrational spacing is much greater in the ground than in the upper state, the increase in $T_{0''}$ should be greater than the increase in $T_{0'}$. The energy difference, T, is therefore expected to decrease with decreasing isotope mass. Thus, the upper state T values for $v' = 0$ appear anomalous and it is not immediately obvious whether the anomaly is in the ground or upper state.

As there are data for the (0, 0), (0, 1) and (1, 0) bands it is possible to separate the isotope effect for each electronic state and determine which of the two states is responsible for the above anomaly. Isotope shifts, $^{i}\Delta T_{v'v''}$, for each band will be defined as the difference between the band origin of each $Ru^{11}B$ isotopologue and that of $^{104}Ru^{11}B$.

$$^{i}\Delta T_{v'v''} = T_{v'v''}(^{i}Ru^{11}B) - T_{v'v''}(^{104}Ru^{11}B) \qquad (5)$$

The difference, $^{i}\delta T\{[18.4]2.5\}$, between the isotope shifts in the (0, 0) and (1, 0) bands will be the difference between the isotope shifts in the $v' = 1$ and 0 levels of the upper [18.4]2.5 state.

Similarly, the difference ${}^{i}\delta T\{X^2\Delta_{5/2}\}$ between the (0, 0) and (0, 1) isotope shifts will give the difference in the ground state, $X^2\Delta_{5/2}$, $v'' = 1$ and 0 shifts.

$$ {}^{i}\delta T\{[18.4]2.5\} = {}^{i}\Delta T_{10} - {}^{i}\Delta T_{00} = {}^{i}\Delta T(v' = 1) - {}^{i}\Delta T(v' = 0) \quad (6) $$

$$ {}^{i}\delta T\{X^2\Delta_{5/2}\} = {}^{i}\Delta T_{00} - {}^{i}\Delta T_{01} = {}^{i}\Delta T(v'' = 1) - {}^{i}\Delta T(v'' = 0) $$

The results are compiled in Table 5.

If the isotope shifts are, as expected, purely due to vibration, the vibrational isotope shift in a given vibrational level will be

$$ (\rho - 1)\omega_e(v + ½) - (\rho^2 - 1)\omega_e x_e(v + ½)^2 \quad (7) $$

and the difference between the $v = 1$ and $v = 0$ isotope shifts will be

$$ {}^{i}\delta T = (\rho - 1)\omega_e - 2(\rho^2 - 1)\omega_e x_e \quad (8) $$

For the ground state, the DFs gave $\omega_e'' \sim 918$ cm^{-1} and $\omega_e x_e'' \sim 4$ cm^{-1}. Upper state vibrational constants could not be determined and we approximate $\omega_e' \sim 675$ cm^{-1} and $\omega_e x_e' \sim 5$ cm^{-1} which would give the observed $\Delta G_{1/2} \sim 665$ cm^{-1}. The results are compared with the observed values in Table 5 and show that there is excellent agreement between observed and calculated values for the ground state but very poor agreement for the excited state. Thus the isotope shift in the ground state is entirely due to the vibrational isotope effect but there appear to be additional interactions affecting the isotope shifts in the $v' = 0$ and possibly also the $v' = 1$ level in the excited state.

As the ground state is regular, the ω_e'' and $\omega_e x_e''$ constants above may be used to calculate the isotope shifts in the ground state. These can then be added to the isotope shifts, ${}^{i}\Delta T_{00}$ and ${}^{i}\Delta T_{10}$, in the (0, 0) and (1, 0) bands to give the individual observed isotope shifts in the $v' = 0$ and 1 levels respectively of the upper state. These can then be compared with vibrational isotope shifts calculated using the upper state vibrational constants ω_e' and $\omega_e x_e'$ above. The results, which are displayed in Table 6, show that the isotope shifts in the $v' = 0$ level are considerably larger than

the pure isotope shift predicted by eq. 7 but that the shifts in the $v' = 1$ level are well represented by eq. 7. Thus the anomaly is purely in the $v' = 0$ level of the [18.4]2.5 state. This is demonstrated in fig. 5, which plots the observed and calculated isotope shifts in the excited state $v' = 0$ and 1 levels and in the ground state $v'' = 0$ level for each Ru isotope. For the $v' = 1$ level, there is a larger difference between observation and calculation only for the $^{99}Ru^{11}B$ isotopologue which has a local perturbation at low J (see below).

(b) Rotation:

As pointed out above, the J', J'' assignment of the observed transitions was straightforward for all RuB isotopologues. For the Ru isotopes of even mass (104, 102, 100, 96), the RuB transitions were single lines which could be fit using the simple polynomial expression (eq, 1) for the rotational energies yielding the molecular constants listed in Tables 2 and 3. The fits were all excellent with no evidence of local perturbations.

For the odd mass (101, 99) Ru isotopes, the RuB transitions showed completely or partially resolved hyperfine structure at low J and broadening of the rotational lines at higher J. The data consisted of individual resolved hyperfine lines at the lowest J values and the low frequency edge (highest F values) of the broadened rotational lines at higher J. These data were fit to the sum of the rotational (eq. 1) and hyperfine (eq. 2) energies yielding also the hyperfine constants, $h_{5/2}$, listed in Tables 2 and 3.

The fits were excellent except for that of the (1,0) band of the $^{99}Ru^{11}B$ isotopologue which was poor, showing signs of a local perturbation in the $v' = 1$ level of the upper state. For this band, the rotational and hyperfine structure were treated separately. The centroids of each broadened line and resolved hyperfine multiplet were taken as the wavenumber of the rotational transition. The rotational energy of the upper state was determined by adding this transition wavenumber to the

ground state energy calculated using the lower state rotational constants of the (0, 0) band. The lowest rotational levels of the [18.4]2.5, $v' = 1$ state are clearly perturbed and the rotational constants were determined only from the unperturbed $J = 5.5 – 9.5$ levels. A reduced term value plot of $T – B[J(J+1) – \Omega^2]$ vs J (fig. 6) shows the perturbation reaching a maximum at $J = 3.5$.

In Table 7, the (Ru) isotopic ratios of B values of each $Ru^{11}B$ isotopologue, relative to that of $^{104}Ru^{11}B$, are compared with the expected value, ρ^2, the inverse ratio of the reduced masses. The agreement is excellent for the ground state and, with the exception of the perturbed $^{99}Ru^{11}B$, good for the upper state $v' = 1$ level. The agreement was not so good for the upper state $v' = 0$ level which suggests that, even though the rotational structure is regular, the interaction described in the previous section, that perturbs this vibrational level, also affects the rotational constants. The agreement for the $Ru^{10}B/Ru^{11}B$ ratios for all the Ru isotopes is excellent in both the ground $v''=0$ and upper state $v' = 1$ levels except for the perturbed ^{99}RuB upper state $v' = 1$ level.

(c) Hyperfine Structure:

The hyperfine constant, $h'_{2.5}$, of the [18.4]2.5 state of $^{99}Ru^{11}B$, listed in table 2, was determined only from the hyperfine structure in the $Q(2.5)$, $P(3.5)$ and $P(4.5)$ transitions with the ground state $h''_{2.5}$ fixed at the value obtained from the (0, 0) band. The ratios $h(^{101}Ru^{11}B)/h(^{99}Ru^{11}B) = 1.060(24)$ for $X^2\Delta_{5/2}(v=0)$, 1.121(17) for [18.4]2.5(v=0) and 1.106(18) for [18.4]2.5(v=1) compare reasonably well with the ratio of the magnetic moments of 1.121.

As discussed by Wang et al. [10], the ground $\Omega = 2.5$ state is the lower spin-orbit component of an inverted $^2\Delta$ state arising from the $(11\sigma)^2(5\pi)^4(2\delta)^3$ configuration. Table 2 of ref [10] listed 3 possible excited configurations and their associated electronic states arising from promotion of a single electron from the ground state. The only states that would have a $\Omega = 2.5$ component were $^2\Phi$ and $^4\Pi$ states arising from the $(11\sigma)^2(5\pi)^4(2\delta)^2(6\pi)^1$ configuration. The excitation would

therefore be from a δ^3 to $\delta^2\pi$ configuration and the spin - allowed transition to the $^2\Phi_{2.5}$ state would seem more probable.

From the molecular orbital diagram in fig. 7, the 2δ orbital is composed entirely of Ru(4dδ) and the 6π orbital is probably a mixture of Ru(4dπ) + B(2pπ). As was the case with CoB [8], the hyperfine structure can provide more insight into the configurational composition of the electronic states. The Frosch and Foley molecular hyperfine parameters [12] cannot be determined from our experimental data but can be calculated using known atomic parameters [14]. The equations for *a*, b_F and *c* are listed in [8]. When the fundamental constants in those equations are converted to appropriate units, the Frosch and Foley parameters, in MHz, are given by the following equations.

$$a/MHz = 95.4128 g_N \frac{1}{\Lambda}\left\langle \Lambda \left| \sum_i \frac{l_{zi}}{r_i^3} \right| \Lambda \right\rangle_l , \quad (9)$$

$$b_F/MHz = 799.3284 g_N \frac{1}{\Sigma}\left\langle \Lambda\Sigma \left| \sum_i s_{zi}\delta_i(r) \right| \Lambda\Sigma \right\rangle_s , \quad (10)$$

$$c/MHz = 143.119 g_N \frac{1}{\Sigma}\left\langle \Lambda\Sigma \left| \sum_i s_{zi} \frac{(3cos^2\theta_i - 1)}{r_i^3} \right| \Lambda\Sigma \right\rangle_s , \quad (11)$$

where $g_N = \mu/I$ (μ is the magnetic moment), r_i is in a.u, l_{zi} and s_{zi} are orbital and spin angular momentum operators for the *i*th electron, δ(r) is a Dirac delta function, and *r* and θ are polar coordinates; the subscripts *l* and *s* indicate different averages which allow for relativistic effects. δ(r) is essentially the electron density at the nucleus which is only nonzero for sσ molecular orbitals. In eq. 7, $(3\cos^2\theta_l - 1)$ = -4/7 for dδ, +2/7 for dπ and -2/5 for pπ orbitals [15].

The magnetic hyperfine matrix elements for a configuration with a single vacancy are equivalent to those for a configuration with a single electron so the open shell configuration reduces to (Ru4dδ) $^2\Delta_{5/2}$ for the ground state and Ru(4dδ)^2 {Ru(4dπ)+B(2pπ)} $^2\Phi_{5/2}$ or $^4\Pi_{5/2}$ for the excited state.

From eq. 4, the expressions for h_Ω become

For $^2\Delta_{5/2}$: $\Lambda = 2$, $\Sigma = +0.5$, $h_{2.5} = 2a + 0.5(b_F + 2c/3)$;

For $^2\Phi_{5/2}$: $\Lambda = 3$, $\Sigma = -0.5$, $h_{2.5} = 3a - 0.5(b_F + 2c/3)$;

For $^4\Pi_{5/2}$: $\Lambda = 1$, $\Sigma = +1.5$, $h_{2.5} = a + 1.5(b_F + 2c/3)$; (12)

The following values are used in the calculations:

^{101}Ru: I = 5/2, μ = -0.7188μ$_N$ [16], g$_N$ = -0.2875μ_N, $\langle r_i^{-3}\rangle$ = 6.145 a.u^{-3}, δ(r) = $|\psi^2(0)|$ = 6.085[14].

^{99}Ru: I = 5/2, μ = -0.6413μ$_N$ [16], g$_N$ = -0.2565μ_N, $\langle r_i^{-3}\rangle$ = 6.145 a.u^{-3}, δ(r) = $|\psi^2(0)|$ = 5.233[14]

^{11}B: I = 3/2, μ = 2.689μ$_N$ [16], g$_N$ = 1.793μ_N, $\langle r_i^{-3}\rangle$ = 0.929 a.u^{-3}, δ(r) = $|\psi^2(0)|$ = 1.775 [14].

Ground State 2δ^3 $^2\Delta_{5/2}$: This configuration involves only the 4dδ orbital associated with the ruthenium atom so there is no contribution to the hyperfine structure from the boron nuclear spin. For ^{101}Ru^{11}B, eqs 9, 10, 11 gave a(Ru) = -0.00562 cm^{-1}, b_F(Ru) = 0 and c(Ru) = +0.00477 cm^{-1}. Eq. 4 then gives $h_{5/2}$(^{101}Ru) = -0.00965 cm^{-1}. The equivalent values for ^{99}Ru^{11}B are a= -0.00502 cm^{-1}, b_F = 0, c = +0.00425 cm^{-1} and h$_{5/2}$(^{99}Ru) = -0.00862 cm^{-1}. These compare with the observed values of $h_{5/2}$ = -0.0071 cm^{-1} for ^{101}Ru^{11}B and -0.0066 cm^{-1} for ^{99}Ru^{11}B. The ~30% difference between the observed and calculated values is reasonable considering the uncertainty about the accuracy of the calculated atomic $\langle r_i^{-3}\rangle$ and $|\psi^2(0)|$ parameters. The above hyperfine calculations indicate that, even if there is some configurational mixing, Ru(4dδ)^3 makes the dominant contribution to the ground state configuration.

Excited State 2δ^{2}6π^1: As pointed out above, this configuration can give $^2\Phi$ and $^4\Pi$ states, both of which have Ω = 2.5 components. The $^2\Phi_{5/2}$ state seems more likely to have a strong transition to the X$^2\Delta_{5/2}$ state but both possibilities will be examined.

$^2\Phi_{5/2}$: For this configuration to give a $^2\Phi$ state, both δ electrons must be in the λ = +2 subshell and must therefore have opposite spins. The π electron must be in the λ = -1 subshell with s = -1/2 to give Λ = 3 and Σ = -1/2. The wavefunction for the $^2\Phi_{5/2}$ component is given by

$$\Psi(^2\Phi_{5/2}) = (2)^{-1/2}\ \{|(\pi_{-1}\beta)(\delta_{+2}\alpha)(\delta_{+2}\beta)| - |(\pi_{-1}\beta)(\delta_{+2}\beta)(\delta_{+2}\alpha)|\}$$

where α and β represent the spin s = +1/2 and -1/2 respectively. This wavefunction is then used in eqs 9, 10 and 11 to give the a, b_F and c parameters. However, the calculated values will depend on the amount of Ru 4dπ and B 2pπ in the 6π orbital. We will examine the extreme cases.

(a) For $^{101}Ru^{11}B$ with the 6π orbital = 100% Ru 4dπ,

a(Ru) = -0.00562 cm^{-1}, b_F(Ru) = 0, c(Ru) = -0.00241 cm^{-1} and $h_{5/2}$(Ru) = -0.0161 cm^{-1}.

(b) For $^{101}Ru^{11}B$ with the 6π orbital = 100% B 2pπ,

a(Ru) = -0.00749 cm^{-1}, b_F(Ru) = 0, c(Ru) = 0 and $h_{5/2}$(Ru) = -0.0225 cm^{-1}.

Experimentally $h_{5/2}$ = -0.0196 cm^{-1} for v' = 0 which is about half way between the 100% Ru and 100% B values so the 6π orbital appears to have significant contributions from both the Ru 4dπ and B 2pπ orbitals. For v' = 1, $h_{5/2}$ = -0.0167 cm^{-1} which suggests that the boron centered orbital plays less part in the configuration of the excited vibrational state.

For situation (a) above only the Ru atom contributes to the hyperfine structure but when the 6π orbital is partially or completely on the B atom there will also be boron hyperfine structure and similar calculations to the above give $h_{5/2}(^{11}B)$ = 0.00531 cm^{-1} for 100% B 2pπ occupancy. This is insufficient to resolve the boron hyperfine structure and results in an almost imperceptible broadening of the Ru hyperfine lines.

The calculations for $^{99}Ru^{11}B$ give (a) $h_{5/2}$(Ru) = -0.0144 cm^{-1} (b) $h_{5/2}$(Ru) = -0.0201 cm^{-1}, $h_{5/2}$(B) = -0.00531cm^{-1}. The experimental value is $h_{5/2}$ = -0.0175 cm^{-1} for v' =0 and -0.0164 cm^{-1} for v' = 1.

$^4\Pi_{5/2}$: To produce a Π state requires one δ electron in each of the λ = +2 and -2 subshells and the π electron in the λ = +1 subshell. The quartet state requires the three spins to be aligned. The wavefunction for the $^4\Pi_{5/2}$ is therefore

$$\Psi(^4\Pi_{5/2}) = |\pi_{+1}\alpha\delta_{+2}\alpha\delta_{-2}\alpha|.$$

(a) For $^{101}Ru^{11}B$ with the 6π orbital = 100% Ru 4dπ,

a(Ru) = -0.00562 cm^{-1}, b_F(Ru) = 0, c(Ru) = +0.00321 cm^{-1}, $h_{5/2}$(Ru) = -0.00321 cm^{-1}

(b) For $^{101}Ru^{11}B$ with the 6π orbital = 100% B 2pπ,

a(Ru) = 0, b_F(Ru) = 0, c(Ru) = +0.00321 cm^{-1}, $h_{5/2}$(Ru) = +0.00321 cm^{-1}.

For $^{99}Ru^{11}B$, $h_{5/2}$(Ru) = (a) -0.00286 cm^{-1} (b) +0.00286 cm^{-1}.

For both isotopologues, $h_{5/2}(^{11}B)$ = +0.00424 cm^{-1}.

Thus, for the $^4\Pi_{5/2}$ state both the Ru and B hyperfine parameters would be too small for the hyperfine structure to be resolved and would, at most, result in a slight broadening of the observed rotational lines. For a Ω = 2.5 upper state from the 2δ6π configuration, only $^2\Phi_{5/2}$ could produce the observed hyperfine structure.

5. Conclusion:

The medium- to low-resolution excitation and dispersed fluorescence experiments, using the pulsed laser, extended the earlier observations [10] to higher vibrational levels in both the excited and ground states. The ground state appeared well behaved and, considering the low resolution (linewidths ~ 5 cm^{-1}), a fit to the vibrational intervals in the DF spectra produced reasonable values for the equilibrium vibrational constants. The vibrational intervals obtained from the band heads in the excitation spectra were irregular. The data in both states were an "average" over all the Ru isotopes which were not resolved.

Our experiments with the cw ring dye laser improved the resolution of the previous experiments [10] by an order of magnitude and, for the first time, resolved the Ru isotope structure and some of the ^{101}RuB and ^{99}RuB hyperfine structure. The rotational analysis confirmed the assignment [10] of the $X^2\Delta_{5/2}$ and [18.4]2.5 states. The vibrational intervals, $\Delta G_{1/2}$, and rotational

constants, B_v, obtained by Wang et al. [10] for both states all fell within the range covered by the Ru isotopic species in Tables 2, 3 and 4.

The Ru isotope ratios and shifts described in the previous section proved very useful in providing more detailed information about the individual vibrational levels in both electronic states. Both the v'' =0 and v'' = 1 ground state vibrational levels were found to be regular and unperturbed and all the isotopologues followed the pattern predicted by the vibrational and rotational isotope effect. The same observation applied to the upper [18.4]2.5 state v = 1 level with the exception of the small local perturbation in the $^{99}Ru^{11}B$ isotopologue. The Ru isotope shifts in the v' = 0 level of the [18.4]2.5 state of all the isotopologues were much larger than predicted by the vibrational isotope effect suggesting interactions with one or more neighboring states. The rotational levels followed a regular pattern but the isotopic B-value ratios for this level were smaller than predicted suggesting an interaction that affected all the rotational levels of this v′ = 0 level.

Analysis of the hyperfine structure provided further insight into the configurational composition of the two electronic states. Comparison of the observed hyperfine parameter $h_{5/2}$ with values calculated using equations 9, 10, 11 and 4 and atomic hyperfine parameters [14] confirmed the previous assumption [10] that the ground $X^2\Delta_{5/2}$ state results primarily from the $(11\sigma)^2(5\pi)^4(2\delta)^3$ configuration where 2δ is the 4dδ orbital centered entirely on the Ru atom. Similar calculations for the [18.4]2.5 state confirmed the previous assignment to the $(11\sigma)^2(5\pi)^4(2\delta)^2(6\pi)^1$ configuration [10] and showed that only the $^2\Phi_{5/2}$ state from this configuration could produce the observed hyperfine structure with the 6π molecular orbital originating from a mixture of Ru4d + B2p atomic orbitals.

The combination of vibrational and rotational analyses with isotope calculations proved a powerful tool for detecting an anomaly in the energy patterns of electronic states and showing that, in the present case, the anomaly originated in the v = 0 level of the [18.4]2.5 state. The hyperfine structure provided insight into the configurational composition of both states. The hyperfine calculations are based on the assumption of a single configuration and the atomic parameters are not always of high precision. Quantitative calculations of the precise compositions of the configurations are not feasible but the present calculations provide useful insights into the primary configurations responsible for the electronic states. There is a need for high level ab initio calculations, especially for the excited states, to facilitate interpretation of future experimental data.

Acknowledgments:

The work described here was supported by grants from the Natural Sciences and Engineering Research Council of Canada. The authors would also like to thank Joyce MacGregor for her laser expertise and help with the experiments.

References

[1] H.-Y. Chung, M. B. Weinberger, J. B. Levine, A. Kavner, J.-M. Yang, S. H. Tolbert, R. B. Kaner, Science 316 (2007) 436-439.

[2] B. Ganem, J. O. Osby, Chem. Rev., 86 (1986), pp. 763-780.

[3] C. Welker, N. S. Phala, J. R. Moss, M. Claeys, E. van Steen, J. Mol. Catal. A Chem. 288 (2008) 75–82.

[4] K. Yamaguchi, N. Mizuno, Angew. Chemie - Int. Ed. 41 (2002) 4538–4542.

[5] K. Grela, S. Harutyunyan, A. Michrowska, Angew. Chemie - Int. Ed. 41 (2002) 4038–4040.

[6] J. A. Tallarico, P. J. Bonitatebus Jr., M. L. Snapper, J. Am. Chem. Soc. 119 (1997) 7157–

7158.

[7] J. V Rau *et al.*, Acta Mater, 57 (2009) 673–681.

[8] J. M. Dore, A. G. Adam, D. W. Tokaryk, C. Linton, J. Mol. Spectrosc. 360 (2019) 44-48.

[9] B. Kharat, S. B. Deshmukh, A. Chaudhari, Int. J. Quantum Chem. 109 (2009) 1103–1115.

[10] N. Wang, Y. W. Ng, A. S. C, Cheung, Chem. Phys. Lett., 547 (2012) 21–23.

[11] C. M. Western, J. Quant. Spectrosc. Radiat. Transf., 186 (2016) 221–242.

[12] R. A. Frosch, H. M. Foley, Phys. Rev., 88 (1952) 1337–1349.

[13] A. Carrington, P. N. Dyer, D. H. Levy, J. Chem. Phys. 47 (1967) 1756-1763.

[14] J. R. Morton, K. F. Preston, J. Magn. Reson., 30 (1978), pp. 577-582.

[15] W. Weltner, Jr., *Magnetic Atoms and Molecules*, (Dover Publications, Inc., New York, 1989)

[16] J.M Brown, A. Carrington, Rotational Spectroscopy of Diatomic Molecules, Cambridge University Press, Cambridge, 2003.

Figure captions:

Fig. 1: Medium-resolution pulsed laser excitation spectrum of RuB. The vibrational assignments of the [18.4]2.5 – $X^2\Delta_{5/2}$ bands are shown. The origin and assignment of all the unmarked bands are presently unknown.

Fig. 2: Dispersed fluorescence spectra showing fluorescence to the $v = 0 – 5$ vibrational levels of the ground $X^2\Delta_{5/2}$ state of $Ru^{10}B$ (top) and $Ru^{11}B$ (bottom) following pulsed laser excitation of the (0, 0) band heads of the [18.4]2.5 – $X^2\Delta_{5/2}$ transition. The lines marked * are transitions to the v = 0 level of another low lying electronic state at ~5996 cm^{-1}.

Fig. 3: High-resolution cw dye laser excitation spectrum of the low J lines in the Q branch of the

(1, 0) band of the [18.4]2.5 – $X^2\Delta_{5/2}$ transition of $Ru^{11}B$. The isotopologue lines from the six Ru isotopes are well separated and clearly observed.

Fig. 4: Observed (top) and calculated (bottom) high resolution spectra of the Q(2.5) transition in the (1, 0) band of the [18.4]2.5 – $X^2\Delta_{5/2}$ transition of $^{101}Ru^{11}B$ showing the hyperfine structure due to the I = 5/2 nuclear spin of ^{11}Ru. The upper labels refer to the more intense $\Delta F = \Delta J = 0$ transitions and the lower labels to the weaker $\Delta F = \pm 1$ lines.

Fig. 5: Observed (symbols) and calculated (solid lines) Ru isotope shifts, relative to ^{104}RuB, in the $v = 0$ and 1 vibrational levels of the [18.4]2.5 state of RuB. The dashed line is the isotope shift in the $v = 0$ level of the $X^2\Delta_{5/2}$ state.

Fig. 6: Reduced term value plot showing the local perturbation in the $v = 1$ level of the [18.4]2.5 state of $^{99}Ru^{11}B$.

Fig. 7: Molecular orbital energy diagram for RuB.z

	$Ru^{11}B$		$Ru^{10}B$	
v	T_v(obs)	obs - calc	T_v(obs)	obs - calc
0	0.0	0.0	0.0	0.0
1	910.3	0.5	949.3	-0.9
2	1811.4	0.0	1892.5	1.7
3	2704.2	-0.4	2821.6	-0.1
4	3589.5	0.0	3741.5	-1.5
5	4466.2	0.1	4655.4	0.8
	ω_e = 918.13(20) $\omega_e x_e$ = 4.15(04)		ω_e = 959.85(87) $\omega_e x_e$ = 4.82(17)	
	σ = 0.31		σ = 1.29	

Table 1. Vibrational energies (cm^{-1}) in the $X^2\Delta_{5/2}$ state of $Ru^{11}B$ and $Ru^{10}B$

Table 2. Molecular constants (in cm^{-1}) of the $Ru^{11}B$ isotopologues determined from the analysis of the [18.4]2.5-$X^2\Delta_{5/2}$ transitions.

State		Isotopologue	T^a	B	10^6D	$h_{5/2}$
$X^2\Delta_{5/2}$	v''=0	$^{104}Ru^{11}B$	0	0.576963(35)	1.36(20)	-
		$^{102}Ru^{11}B$	0	0.578050(30)	1.17(17)	-
		$^{101}Ru^{11}B$	0	0.578516(27)	0.84(25)	-0.00709(26)
		$^{100}Ru^{11}B$	0	0.579177(33)	0.82(22)	-
		$^{99}Ru^{11}B$	0	0.579636(16)	0.61(16)	-0.00669(14)
		$^{96}Ru^{11}B$	0	0.581543(51)	1.28(39)	-
	v''=1	$^{104}Ru^{11}B$	909.7865(11)	0.573098(61)	1.76(44)	-
		$^{102}Ru^{11}B$	910.6315(9)	0.574257(43)	2.34(35)	-
		$^{101}Ru^{11}B$	-	-	-	-
		$^{100}Ru^{11}B$	911.5144(9)	0.575185(28)	-	-
		$^{99}Ru^{11}B$	-	-	-	-
		$^{96}Ru^{11}B$	-	-	-	-
[18.4]2.5	v'=0	$^{104}Ru^{11}B$	18444.0698(7)	0.502214(40)	2.16(24)	-
		$^{102}Ru^{11}B$	18444.1699(6)	0.502995(28)	1.38(15)	-
		$^{101}Ru^{11}B$	18444.2245(3)	0.503328(26)	0.86(19)	-0.01960(25)
		$^{100}Ru^{11}B$	18444.2931(6)	0.503781(34)	0.64(22)	-
		$^{99}Ru^{11}B$	18444.3617(2)	0.504070(16)	0.17(11)	-0.01749(15)
		$^{96}Ru^{11}B$	18444.6300(8)	0.505371(51)	0.85(34)	-
	v'=1	$^{104}Ru^{11}B$	19109.8185(7)	0.496263(44)	1.93(28)	-
		$^{102}Ru^{11}B$	19110.3123(6)	0.497216(31)	2.00(15)	-
		$^{101}Ru^{11}B$	19110.5640(3)	0.497668(26)	2.08(19)	-0.01665(27)
		$^{100}Ru^{11}B$	19110.8337(6)	0.498302(37)	2.93(24)	-
		$^{99}Ru^{11}B$	19111.1747(47)	0.497017(200)	-6.9(1.5)	-0.01506(11)
		$^{96}Ru^{11}B$	19111.9291(9)	0.499875(73)	10.78(82)	-

[a] $T(v''=0)$ is fixed at 0 cm^{-1} for all isotopologues.

Table 3. Molecular constants (in cm^{-1}) of the $Ru^{10}B$ isotopologues determined from the analysis of the [18.4]2.5-$X^2\Delta_{5/2}$ transitions.

State		Isotopologue	T^a	B	10^6D	$h_{5/2}$
$X^2\Delta_{5/2}$	v''=0	$^{104}Ru^{10}B$	0	0.628663(32)		
		$^{102}Ru^{10}B$	0	0.629640(28)		
		$^{101}Ru^{10}B$	0	0.630400(22)	2.49(39)	-0.0072(2)
		$^{100}Ru^{10}B$	0	0.630786(28)		
		$^{99}Ru^{10}B$	0	0.631611(90)	9.3(2.4)	-0.0065(6)
		$^{96}Ru^{10}B$	0	0.633140(36)		
[18.4]2.5	v'=1	$^{104}Ru^{10}B$	19128.1934(4)	0.540356(25)	1.27(07)	
		$^{102}Ru^{10}B$	19128.6778(5)	0.541306(31)	1.43(12)	
		$^{101}Ru^{10}B$	19128.9243(1)	0.541930(21)	2.63(30)	-0.01668(2)
		$^{100}Ru^{10}B$	19129.1803(4)	0.542273(25)	0.66(13)	
		$^{99}Ru^{10}B$	19129.4363(5)	0.542886(79)	4.2(1.4)	-0.01506(52)
		$^{96}Ru^{10}B$	19130.2331(5)	0.544542(35)	1.99(29)	

[a] T'' if fixed at 0 for all isotopologues

Table 4. Vibrational separations ${}^{i}\Delta G_{1/2}$ (cm^{-1}) and isotopic ratios in the $X^2\Delta_{5/2}$ and [18.4]2.5 states of ${}^{i}Ru^{11}B$ isotopologues

	$X^2\Delta_{5/2}$		[18.4]2.5		
i	${}^{i}\Delta G_{1/2}$	${}^{i}\Delta G_{1/2}/{}^{104}\Delta G_{1/2}$	${}^{i}\Delta G_{1/2}$	${}^{i}\Delta G_{1/2}/{}^{104}\Delta G_{1/2}$	ρ
104	909.7865	1.00000	665.7487	1.00000	1.00000
102	910.6315	1.00093	666.1424	1.00059	1.00094
101			666.3395	1.00089	1.00142
100	911.5148	1.00190	666.5402	1.00119	1.00192
99			666.8097	1.00159	1.00242
96			667.2991	1.00233	1.00399

Table 5. Observed and calculated difference between the $v = 1$ and 0 isotope shifts (in cm^{-1}) in each of the [18.4]2.5 and $X^2\Delta_{5/2}$ states of $^{i}Ru^{11}B$

	Isotope Shift			[18.4]2.5		$X^2\Delta_{5/2}$	
i	(0,0)	(1,0)	(0,1)	(1,0) - (0,0)	calc	(0,0) - (0,1)	calc
104	0	0	0	0	0	0	0
102	0.100	0.494	-0.745	0.394	0.625	0.845	0.848
101	0.155	0.746		0.591	0.946		
100	0.224	2.015	-1.505	0.791	1.275	1.729	1.729
99	0.292	1.353		1.061	1.608		
96	0.560	2.111		1.551	2.651		

Table 6. Isotope shifts (cm^{-1}) in the $X^2\Delta_{5/2}$ $v = 0$ and [18.4]2.5 $v = 0$ and 1 states of $Ru^{11}B$

	$X^2\Delta_{5/2}$ $v = 0$		[18.4]2.5 $v = 0$		[18.4]2.5 $v = 1$
i	calc	obs	calc	obs	calc
104	0	0	0	0	0
102	0.430	0.530	0.315	0.923	0.931
101	0.650	0.805	0.477	1.396	1.409
100	0.876	1.100	0.642	1.891	1.897
99	1.105	1.397	0.810	2.458	2.394
96	1.822	2.382	1.336	3.933	3.947

Table 7. Observed and calculated isotopic ratios of rotational constants, B_v, of RuB

[a] Upper entry $v = 0$; Lower entry $v = 1$

	$B_v(^{i}Ru^{11}B)/B_v(^{104}Ru^{11}B)$			$B_v(^{i}Ru^{10}B)/B_v(^{i}Ru^{11}B)$		
i	$X^2\Delta_{5/2}(v=0)$	[18.4]2.5[a]	ρ^2	$X^2\Delta_{5/2}(v=0)$	[18.4]2.5(v=1)	ρ^2
104	1.00000	1.00000 1.00000	1.00000	1.0896	1.0889	1.0900
102	1.00188	1.00156 1.00192	1.00188	1.0892	1.0887	1.0898
101	1.00269	1.00222 1.00283	1.00285	1.0884	1.0889	1.0897
100	1.00384	1.00311 1.00411	1.00384	1.0891	1.0882	1.0896
99	1.00463	1.00361 1.00188	1.00484	1.0898	1.0919	1.0895
96	1.00794	1.00629 1.00728	1.00799	1.0887	1.0894	1.0893

Graphical abstract

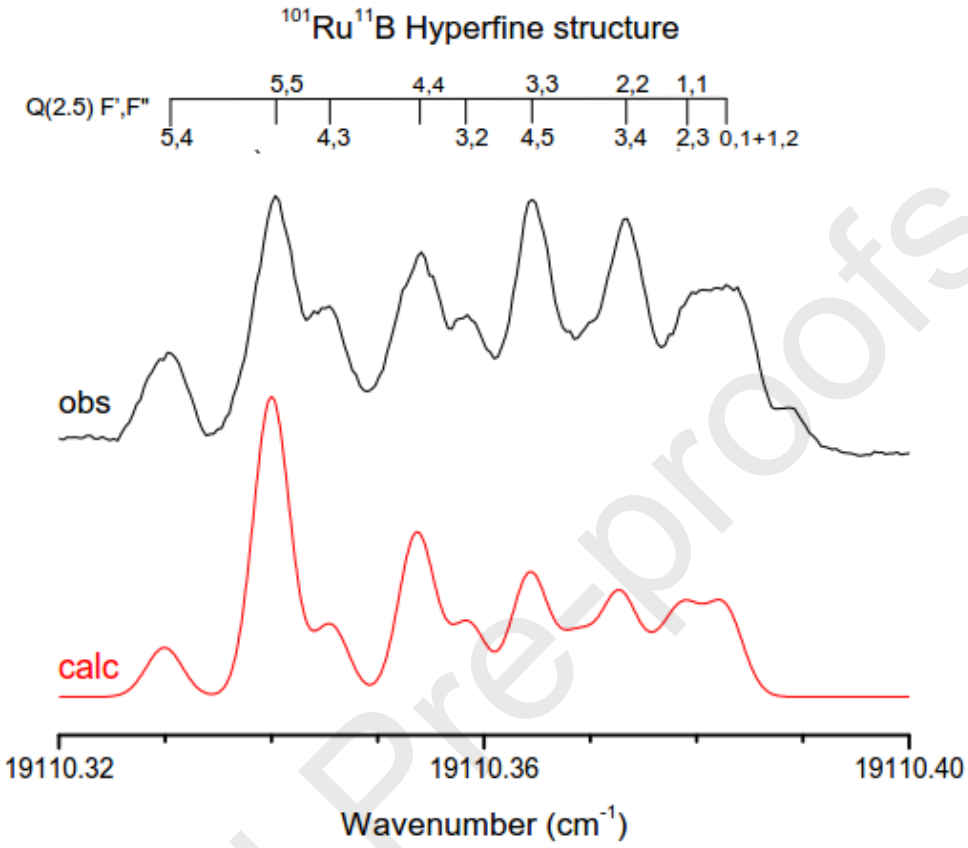

Highlights:

Resolved 12 RuB isotopologues and ^{99}RuB and ^{101}RuB hyperfine structure
Analysis of Ru isotope structure reveal anomalies in v=0 level of excited state
Rotational analysis confirms Ω=2.5 assignment of both electronic states
Hyperfine constants yield insights into electron configuration of both states